Phase diagram and domain splitting in thin ferroelectric films with incommensurate phase

A. N. Morozovska,[1,*,†] E. A. Eliseev,[1,2] JianJun Wang,[3] G. S. Svechnikov,[1] Yu. M. Vysochanskii,[4] Venkatraman Gopalan,[3] and Long-Qing Chen[3,*,‡]

[1]*V. Lashkarev Institute of Semiconductor Physics, NAS of Ukraine, prospect Nauki 41, 03028 Kiev, Ukraine*

[2]*Institute for Problems of Materials Science, NAS of Ukraine, Krjijanovskogo 3, 03142 Kiev, Ukraine*

[3]*Department of Materials Science and Engineering, Pennsylvania State University, University Park, Pennsylvania 16802, USA*

[4]*Institute for Solid State Physics and Chemistry, Uzhgorod University, 88000 Uzhgorod, Ukraine*

(Received 23 December 2009; revised manuscript received 25 April 2010; published 27 May 2010)

We studied the phase diagram of thin ferroelectric films with incommensurate phases and semiconductor properties within the framework of Landau-Ginzburg-Devonshire theory. We performed both analytical calculations and phase-field modeling of the temperature and thickness dependencies of the period of incommensurate 180°-domain structures appeared in thin films covered with perfect electrodes. It is found that the transition temperature from the paraelectric into the incommensurate phase as well as the period of incommensurate domain structure strongly depend on the film thickness, depolarization field contribution, surface and gradient energy. The results may provide insight on the temperature dependence of domain structures in nanosized ferroics with inherent incommensurate phases.

DOI: 10.1103/PhysRevB.81.195437 PACS number(s): 77.80.Dj, 64.70.Rh

I. INTRODUCTION

The incommensurate phase in bulk materials is the spatially modulated state with period incommensurate with the lattice constant.[1] The spontaneous modulation appears when the homogeneous state is either unstable or less energetically preferable (metastable). On the other hand, the initial homogenous states could become modulated in the spatially confined systems. Typical examples are domain structures of either ferroelectric or ferromagnetic films due to the depolarization or demagnetization fields, respectively.

The influence of surfaces and interfaces on ferroic materials polar properties and their domain structure have been attracting much attention since early seventies till the present.[2–8] Laminar domain structure formation in thick films with free surfaces was considered in the classic papers by Kittel[9] for ferromagnetic media and Mitsui and Furuichi[10] for ferroelectric media. The structure of a single boundary between two domains in the bulk ferroelectrics was considered by Cao and Cross[11] and Zhirnov,[12] allowing for electrostriction contribution. Formation and stability of ferroelastic domain structures were considered by different groups.[13–15]

The development of nonvolatile ferroelectric memory technology has rekindled the interest in ferroelectric properties and polarization reversal mechanisms in ultrathin films.[16–19] One of the key parameters controlling ferroic behavior is the structure and energetic of domain walls.

The wall behavior at surfaces and interfaces will determine polarization switching and pinning mechanisms. Under the absence of external fields in the bulk, the 180°-domain wall is not associated with any depolarization effects. However, the symmetry breaking on the wall-surface or wall-interface junction can give rise to a variety of unusual effects due to the depolarization fields across the wall, as determined by screening mechanisms and strain boundary conditions.[20] For instance, density-functional theory results predicted the stabilization of vortex structure in ferroelectric nanodots under the transverse inhomogeneous static electric field.[21,22] This prediction has resulted in extensive experimental efforts to discover toroidal polarization states in ferroelectrics.[23,24]

However, despite numerous studies, size and surface effect on domain walls behavior in ferroics is still not clear. Much remained to be done to clarify the peculiarities of the order parameter redistribution in the wall vicinity and corresponding wall energy in confined systems like thin films and nanoparticles. For instance, simple analytical models typically face with "Kittel paradox:" 180-degree "rigid" domain structure with ultra-sharp walls produces extra-high depolarization fields near unscreened surface.[25] Possible formation of closure domains in rigid ferroelectrics with infinitely thin domain walls does not solve the problem. Relevant analytical treatment of multiaxial polarization switching allowing for domain walls intrinsic widths is still underway due to the numerous obstacles. At the same time both first principle calculations and phenomenological modeling revealed unusual domain structures in different ferroelectrics,[26,27] resembling domain structures typical for ferromagnetics.

The axial next-nearest-neighbor Ising (ANNNI) model was successfully applied to study of the size effect on the properties of magnetic films by W. Selke *et al.*[28,29] The sequence of the ordered phases for different film thickness and the couplings in the surface layers obtained from mean-field theory, Monte Carlo simulations, and low-temperature expansions was analyzed.

However the applicability of ANNNI model to the thin ferroelectric films with out-of-plane polarization is questionable, since the effect of strong depolarization field (dipole-dipole interactions) not considered within the model, while it is of great importance for out-of-plane polarization geometry.[30] On the other hand continuum Landau-Ginzburg-Devonshire (LGD) models naturally involve depolarization field and allow analytical calculations for spatially confined ferroelectrics. Despite the remark, results obtained within the ANNI model (as well as in others discrete and atomistic models) should call for care when using continuum theory in the thin films.

Since the exchange forces are prevailing ones for the ferromagnetic systems, the magnetic dipole-dipole interaction is often omitted under the theoretical consideration of these systems. However dipole—dipole interaction strongly affects the anisotropy energy of magnetic nanoparticles (see, e.g., Ref. 31). Unfortunately in the discrete model framework the efforts to compute the dipole-dipole interaction energy drastically increase with the increase of spins quantity (see, e.g., Ref. 32). In this case the continuum limit model could present the simple picture of the system behavior without the necessity to make huge efforts and involve complicated calculation schemes.

Thus, the elaboration of the continuum LGD model seems especially important for considered case of the thin ferroelectric films with incommensurate phase, since the consistent calculations with all necessary details included was virtually absent. Possibly it is due to the fact the situation with the theoretical description of the incommensurate ferroelectrics is much more complex in comparison with the commensurate ones. In particular within Landau phenomenological approach of the II-type incommensurate materials, the characteristics of modulated phase should be found from forth order nonlinear Euler-Lagrange differential equations (see, e.g., Refs. 33–35); for commensurate ferroelectrics the equations are of the second order. Owing to the problem complexity only few papers were published within oversimplified LGD-model. Namely, Charnaya *et al.*[36] obtained the order parameter distribution over the film thickness using the assumption of slowly-varying amplitude and considered the effect of size on the temperature of the phase transition into the incommensurate phase. The direction of incommensurate phase modulation was normal to the film plane, but the depolarization field was not considered, while the depolarization field becomes inevitable present in the system.

The most intriguing feature is the mechanism of commensurate-incommensurate phase transitions. The transition in three-dimensional solids was considered as lock-in transition from the incommensurate phase with negative energy of domain walls into the commensurate phase with positive energy of domain walls.[37] Levanyuk *et al.* pointed out that electrostriction coupling between polarization and strains significantly changes the phase equilibrium.

The link between the phenomenological model of incommensurate crystals and quasimicroscopic discrete lattice model was established in Ref. 38. The temperature dependence of the polarization wave number in ferroelectric $Sn_2P_2Se_6$ as well as the anomalous heat capacity in the incommensurate phase were explained in the framework of II-type phenomenological theory using the nonharmonic distribution of the order parameter.[35] First-principle calculations[39] may pour light of the local structure of the incommensurate ferroelectrics, however their realization for confined systems like thin films are almost not evolved to date.

Possible pitfall of LGD theory application for the spatially confined incommensurate ferroelectrics is the applicability of the continuum media theory to nanosized systems. For nanosized ferroics the applicability of LGD theory is corroborated by the fact that the critical sizes of the long-range order appearance calculated from discrete atomistic[40–43] and phenomenological[5,44,45] theories are in a good agreement with each other as well as with experimental results for ferromagnetic[46] and ferroelectric[16,47–50] systems.

The paper is devoted to the size effects in thin ferroelectric films with incommensurate phase and organized as follows. Section II is the problem statement. Here we listed expressions for the depolarization field and the free energy functional of ferroelectric thin films with II-type incommensurate phase and semiconductor properties. Approximate analytical solution of the Euler-Lagrange equations is presented in Sec. III. Results of the analytical calculations of the size effect on phase equilibrium and domain structure temperature evolution are discussed in Secs. IV and I. Sections IV and II contains results obtained by phase-field modeling. Last section is a brief summary.

II. PHENOMENOLOGICAL DESCRIPTION OF THE FERROELECTRIC THIN FILMS WITH THE II-TYPE INCOMMENSURATE PHASE

Let us consider a film of incommensurate ferroelectric with semiconductor properties. The spontaneous polarization P_3 is directed along the polar axis z. The sample is dielectrically isotropic in transverse directions, i.e., permittivity $\varepsilon_{11}=\varepsilon_{22}$ at zero external field.

Further we assume that the dependence of in-plane polarization components on $E_{1,2}$ can be linearized as $P_{1,2}\approx\varepsilon_0(\varepsilon_{11}-1)E_{1,2}$ (ε_0 is the universal dielectric constant). Thus the polarization vector acquires the form: $\mathbf{P}(\mathbf{r})=[\varepsilon_0(\varepsilon_{11}-1)E_1,\varepsilon_0(\varepsilon_{11}-1)E_2,P_3(\mathbf{E},\mathbf{r})+\varepsilon_0(\varepsilon_{33}-1)E_3]$.[51] Maxwell's equations for the inner electric field $\mathbf{E}_i=-\nabla\varphi_i(\mathbf{r})$, expressed via electrostatic potential $\varphi_i(\mathbf{r})$ and polarization $\mathbf{P}(\mathbf{r})$ reduces to the equation $\frac{\partial^2\varphi_i}{\partial z^2}+\frac{\varepsilon_{11}}{\varepsilon_{33}}\left(\frac{\partial^2\varphi_i}{\partial x^2}+\frac{\partial^2\varphi_i}{\partial y^2}\right)-\frac{\varphi_i}{\varepsilon_{33}R_d^2}=\frac{1}{\varepsilon_0\varepsilon_{33}}\frac{\partial P_3}{\partial z}$, R_d is the Debye screening radius. A background permittivity ε_{33} is regarded much smaller than ferroelectric contribution to temperature-dependent permittivity ε_{33}^f.

The boundary conditions $\varphi_i(x,y,0)=\varphi_e(x,y,0)$, $\varphi_i(x,y,h)=0$ used hereinafter correspond to the full screening of depolarization field outside the sample that is realized by the ambient charges or perfect electrodes; h is the film thickness.

In Debye approximation the Fourier representation on transverse coordinates $\{x,y\}$ for the depolarization field E_3^d has the form (see Appendix A in Ref. 52 for details)

$$\tilde{E}_3^d[\tilde{P}_3(\mathbf{k},z)]=\left\{-\frac{\tilde{P}_3(\mathbf{k},z)}{\varepsilon_0\varepsilon_{33}}+\int_0^z dz'\tilde{P}_3(\mathbf{k},z')\cosh(Kz')\frac{\cosh[K(h-z)]}{\varepsilon_0\varepsilon_{33}\cdot\sinh(Kh)}K+\int_z^h dz'\tilde{P}_3(\mathbf{k},z')\cosh[K(h-z')]\frac{\cosh(Kz)K(k)}{\varepsilon_0\varepsilon_{33}\cdot\sinh(Kh)}\right\}. \quad (1)$$

Here vector $\mathbf{k}=\{k_1,k_2\}$, its absolute value $k=\sqrt{k_1^2+k_2^2}$, func-

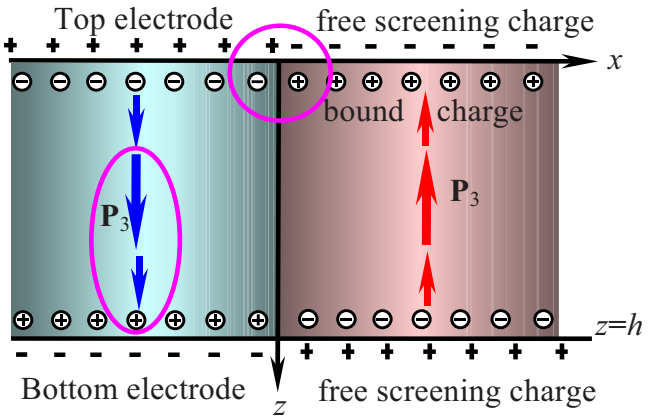

FIG. 1. (Color online). 180°-domain structure of thin film covered with perfect electrodes. Break of double electric layers at the film-surface junction (marked by a circle) and polarization inhomogeneity (arrows of different length) cause depolarization field.

tion $K(k)=\sqrt{(\varepsilon_{11}k^2+R_d^{-2})/\varepsilon_{33}}$. For the dielectric media with polarization $P_3(z)$ independent on x,y coordinates and $R_d \to \infty$ expression (1) reduces to the expression for depolarization field obtained by Kretschmer and Binder.[2]

Figure 1 schematically illustrates the origin of depolarization fields in thin films with 180°-domain structure and inhomogeneous polarization component $P_3(x,z)$. Depolarization field $\mathbf{E}_i^d$ is caused by imperfect screening of the bound polarization charges by the surrounding, inhomogeneous polarization distribution and/or its breaks at interfaces. Mathematically it arises once div $\mathbf{P} \neq 0$.

Correct phenomenological description of a nanosized system requires the consideration of its surface energy F_S. Including the surface energy term, LGD free-energy $F=F_S+F_V$ depends on the chosen order parameter—spontaneous polarization component P_3.

Within the LGD theory for the II-type incommensurate materials the spatial distribution of the spontaneous polarization component P_3 inside the film of thickness h could be found by the minimization of the free-energy functional (see e.g., Refs. 45 and 53)

$$F \approx \int_0^h dz \int_{-\infty}^{\infty} dxdy \left[\frac{\alpha'}{2}P_3^2 + \frac{\beta'}{4}P_3^4 + \frac{\gamma}{6}P_3^6 - P_3\left(\frac{E_3^d}{2} + E_3^e\right) + \frac{g_i}{2}\left(\frac{\partial P_3}{\partial x_i}\right)^2 + \frac{w_i}{2}\left(\frac{\partial^2 P_3}{\partial x_i^2}\right)^2 + \frac{v_i}{2}\cdot P_3^2\left(\frac{\partial P_3}{\partial x_i}\right)^2 \right] + \frac{\alpha^S}{2}\int_{-\infty}^{\infty} dxdy(P_3^2|_{z=0} + P_3^2|_{z=h}). \quad (2)$$

Coefficient $\alpha(T)=\alpha_T(T-T_C)$ explicitly depends on temperature T, T_C is the Curie temperature of a bulk material.

For thin films coefficients $\alpha'(T)$ and β' should be renormalized due to the electrostriction coupling as shown by Cao and Cross[12] and Zhirnov[11] and misfit strain originated from the film and substrate lattice mismatch,[54,55] as $\alpha' = \alpha(T) - \frac{(Q_{11}+Q_{12})u_m^*}{s_{11}+s_{12}} - 2\frac{(Q_{11}^2+Q_{12}^2)s_{11}-2s_{12}Q_{11}Q_{12}}{s_{11}^2-s_{12}^2}\bar{P}_0^2$ and $\beta' = \beta + 2\frac{(Q_{11}^2+Q_{12}^2)s_{11}-2s_{12}Q_{11}Q_{12}}{s_{11}^2-s_{12}^2}$, where s_{ij} is the elastic compliances tensor at constant polarization; Q_{ij} is the electrostriction tensor, α and β are stress-free expansion coefficients, the average spontaneous polarization is $\bar{P}_0$,[56] u_m^* is the *effective* misfit strain, at that $u_m^*(L) \approx u_m$, $L \leq h_d$ and $u_m^*(L) \approx u_m h_d/L$, $L > h_d$ (h_d is the critical thickness of dislocations appearance) in accordance with the model proposed by Speck and Pompe.[57] The epitaxial strain $u_m=(a/c)-1$ originated from the thin film (a) and substrate (c) lattice constants mismatch.

The gradient coefficient g_i and seeding coefficient β could be negative, other higher coefficients are positive. Last integral term in Eq. (2) is the surface contribution to the system free energy. Expansion coefficients of the polarization-dependent surface energy may be different for different surface regions. Below we approximate the coordinate dependence by effective value α^S and neglect higher order terms in the surface energy. The depolarization field E_3^d is given by Eq. (1).

The *necessary condition* of the incommensurate phase appearance, $g_i<0$, should be satisfied at least in one spatial direction (i.e., for one value of i), while for other directions the homogeneous state would be stable if $g_j>0$. Since most of ferroelectrics with incommensurate phase are uniaxial or biaxial ones, the coefficients g_i are not necessarily equal. In order to simplify our consideration and obtain close-form analytical results, we suppose that $g_3>0$ and either $g_1=g_2<0$ (symmetric biaxial x,y-incommensurate case) or $g_1<0$ & $g_2>0$ (uniaxial x-incommensurate case). In this case one could neglect the higher order derivatives on z and put $w_3=0$ and $v_3=0$ in Eq. (2). Coefficients w_1 and v_1 should be nonzero positive values for the x-incommensurate modulation existence; or coefficients $w_1=w_2$ and $v_1=v_2$ should be nonzero positive values for the x,y-incommensurate modulation existence. This simplified model allows analytical consideration of the influence of size effects, depolarization field and surface energy on the incommensurate phase features.

So, under the conditions $g_1=g_2<0$, $w_1=w_2$ and $v_1=v_2$, $g_3>0$ and $w_3=0$ and $v_3=0$, minimization of the free-energy (2) results into the relaxation equation for polarization distribution

$$\Gamma\frac{\partial P_3}{\partial t} + \alpha'(T)P_3 + \beta' P_3^3 + \gamma P_3^5 - g_3\frac{\partial^2 P_3}{\partial z^2} - (g_1 + v_1 P_3^2)\left(\frac{\partial^2 P_3}{\partial x^2} + \frac{\partial^2 P_3}{\partial y^2}\right) + w_1\left(\frac{\partial^4 P_3}{\partial x^4} + \frac{\partial^4 P_3}{\partial y^4}\right) - v_1 P_3\left[\left(\frac{\partial P_3}{\partial x}\right)^2 + \left(\frac{\partial P_3}{\partial y}\right)^2\right] = E_3^d(x,y,z) + E_0^e \exp(i\omega t), \quad (3)$$

where Γ is a positive relaxation coefficient, ω is the frequency of external field E_0^e. For 1D case one should put $\partial P_3/\partial y=0$ and consider $P_3(x,z)$ in Eq. (3). The important feature of the Eq. (3) is depolarization field E_3^d that nonlocally depends on $P_3(x,y,z)$ as given by the linear integral operator in Eq. (1).

The boundary conditions for polarization acquire the form

$$\left(\alpha^S P_3 - g_3\frac{\partial P_3}{\partial x_3}\right)\Bigg|_{x_3=0} = 0, \quad \left(\alpha^S P_3 + g_3\frac{\partial P_3}{\partial x_3}\right)\Bigg|_{x_3=h} = 0. \tag{4}$$

Similarly to the case of commensurate ferroelectrics one could introduce extrapolation length $\Lambda = g_3/\alpha^S$ that is usually positive. Infinite extrapolation length corresponds to an ideal surface ($\alpha^S \to 0$) and so-called natural boundary conditions, while zero extrapolation length ($\alpha^S \to \infty$) corresponds to $P_3(x_3=0)=0$ at a strongly damaged surface without long-range order. Reported experimental values are $\Lambda = 2-50$ nm.[58,59]

III. APPROXIMATE ANALYTICAL SOLUTION OF THE EULER-LAGRANGE EQUATIONS

Then one could find the solution of Eq. (3) linearized for the small polarization modulation $p(\mathbf{k},z)$ in the form of series on the eigen functions $f_n(k,z)$

$$p(\mathbf{k},z,t) = \sum_n \left[A_n(\mathbf{k}) f_n(k,z) \exp\left(-\lambda_n(k)\frac{t}{\Gamma}\right) + E_n(\mathbf{k},\omega)\frac{f_n(k,z)\exp(i\omega t)}{\lambda_n(k) + i\omega\Gamma}\right]. \tag{5}$$

Hereinafter $k=|\mathbf{k}|$ and $\mathbf{k}=\{k_x,k_y\}$ for the x,y-incommensurate modulation or $\mathbf{k}=\{k_x,0\}$ for the x-incommensurate modulation.

The first term in Eq. (5) is related to the relaxation of initial conditions while the second one is the series expansion external stimulus $\tilde{E}_0^e$ via the eigen functions $f_n(k,z)$. The eigen functions $f_n(k,z)$ and eigen values $\lambda_n(k)$ should be found from the nontrivial solutions of the following problem:

$$\left[\alpha^* - g_3^*\frac{d^2}{dz^2} + g_1^* k^2 + w_1 k^4\right] f_n(k,z) - E_3^d[f_n(k,z)] = \lambda_n(k) f_n(k,z), \tag{6a}$$

$$\left(\alpha^S f_n - g_3\frac{\partial f_n}{\partial z}\right)\Bigg|_{z=0} = 0, \quad \left(\alpha^S f_n + g_3\frac{\partial f_n}{\partial z}\right)\Bigg|_{z=h} = 0, \tag{6b}$$

where $\alpha^* = \alpha' + 3\beta\bar{P}_0^2 + 5\gamma\bar{P}_0^4$, $g_1^* = g_1 + v_1\bar{P}_0^2$ and $\bar{P}_0$ is the average polarization (for a bulk single domain sample the spontaneous polarization $P_0^2 = (\sqrt{\beta^2 - 4\alpha\gamma} - \beta)/2\gamma$). Depolarization field $E_3^d[f_n(k,z)]$ given by integral operator (1) and involved into the problem (6) determines the solution form.

Note, that the linear harmonic approximation is valid in the paraelectric phase as well as in it's the immediate vicinity, where ferroelectric nonlinearity can be neglected.

The solution of Eq. (6) was derived as (see Appendix A in Ref. 52 for details)

$$f_n(k,z) \sim \cosh\left[q_{n1}\left(\frac{z}{h} - \frac{1}{2}\right)\right] - \frac{q_{n2}^2 - h^2K^2}{q_{n1}^2 - h^2K^2}\frac{q_{n1}\sinh(q_{n1}/2)}{q_{n2}\sinh(q_{n2}/2)}\cosh\left[q_{n2}\left(\frac{z}{h} - \frac{1}{2}\right)\right]. \tag{7}$$

Here $q_{n1,2}$ are expressed via the eigen value λ_n as the solutions of the biquadratic equation

$$\alpha^* + g_1^* k^2 + w_1 k^4 - g_3\frac{q_n^2}{h^2} + \frac{q_n^2}{\varepsilon_0\varepsilon_{33}(q_n^2 - h^2K^2)} = \lambda_n(k). \tag{8}$$

The equation for the eigen spectrum $\lambda_n(k)$ is

$$\frac{q_{n1}\sinh(q_{n1}/2)}{q_{n1}^2 - h^2K^2} = \frac{q_{n2}\sinh(q_{n2}/2)}{q_{n2}^2 - h^2K^2}\left(\frac{\cosh(q_{n1}/2)(\alpha^S/g_3) + (q_{n1}/h)\sinh(q_{n1}/2)}{\cosh(q_{n2}/2)(\alpha^S/g_3) + (q_{n2}/h)\sinh(q_{n2}/2)}\right). \tag{9}$$

Note, that similar equations could be found for "sinh"-eigen functions. Since the smallest (first) eigenvalue should correspond to eigen function of constant sign, we restrict our consideration for the first symmetric "cosh"-eigen functions (7).

The equilibrium dependence of the transverse modulation wave vector k on the temperature T and film thickness h should be found from Eqs. (8) and (9) under the conditions $\lambda_{\min}=0$.

IV. SIZE EFFECT ON THE PHASE EQUILIBRIUM AND DOMAIN STRUCTURE TEMPERATURE EVOLUTION

A. Harmonic approximation

Transcendental Eq. (9) was essentially simplified at the domain structure onset (see Appendix B in Ref. 52) so that the approximate expression for the highest and lowest roots was derived in the form

$$k_\pm^2(h,T) \approx -\frac{g_1^*}{2w_1} \pm \sqrt{\frac{g_1^{*2}}{4w_1^2} - \frac{1}{w_1}\left(\alpha^*(T) + \frac{2\alpha^S g_3}{(\alpha^S\sqrt{g_3\varepsilon_0\varepsilon_{33}} + g_3)h + \alpha^S g_3\varepsilon_0 h^2/4R_d^2}\right)}. \tag{10}$$

Note, that the size-dependent term in Eq. (10), $\frac{2\alpha^S g_3}{(\alpha^S\sqrt{g_3\varepsilon_0\varepsilon_{33}}+g_3)h+\alpha^S g_3\varepsilon_0 h^2/4R_d^2}$, originates from the influence of depolarization field given by Eq. (1) and the finite surface energy ($\alpha^S \neq 0$). The finite-size effect is absent only for the unrealistic case without surface energy, when $\alpha^S=0$. Under the typical conditions $R_d \gg 50$ nm and $g_3 \sim 10^{-10}$ J·m^3/C^2, the term $\alpha^S g_3\varepsilon_0 h^2/4R_d^2$ can be neglected in the denominator of Eq. (10) without any noticeable loss of precision. For the particular case the depolarization term is proportional to $1/h$ as anticipated for ferroelectrics dielectrics.[2,20,53,54] The depolarization effect vanishes with the film thickness increase ($h \to \infty$).

The root $k_-(h,T)$ is always stable only in the incommensurate phase of the bulk material. The root $k_+(h,T)$ can be (meta)stable in thin films even in the temperature range corresponding to the bulk commensurate phase, since domain stripes with definite period correspond to smaller depolarization field in comparison with a single domain distribution. The direct comparison of the corresponding free energies (2) should be performed in order to determine the film thickness range, where the roots $k_\pm(h,T)$ are stable (and thus single domain distribution is unstable).

The comparison of the free energies (2) was performed in harmonic approximation. It was demonstrated that the root $k_+(h,T)$ can be stable in the wide temperature range starting from the low temperatures (much smaller than T_C) the up to the vicinity of the transition temperature into the paraelectric phase. This striking result can be explained in the following way. A single domain state should be energetically preferable in the commensurate ferroelectric defect-free film placed between perfect conducting electrodes, but only for the case of zero surface energy (coefficient $\alpha^S=0$, $\Lambda \to \infty$). Even under the absence of defects domain stripes originate from imperfect screening of depolarization field outside the film (either imperfect electrodes, dielectric gap) and/or the spatial confinement (i.e., surface energy contribution determined by nonzero α^S). Zero value of α^S means natural boundary conditions and the absence of finite size and depolarization effects, since the polarization is homogeneous along the polar axis and the depolarization field is absent for the case. The nonzero values α^S lead to appearance of polarization inhomogeneity along the polar axis, localized near the surfaces. At the same time, inhomogeneity along the polar axis should induce the depolarization field that affects periodically modulated domain structures. This effect is a general feature of all ferroics (see e.g., Refs. 53 and 60), it is not related with a bulk incommensurate phase.

The value $\bar{P}_0 \to 0$ in the vicinity of the transition from the paraelectric into modulated ferroelectric phase, while $\bar{P}_0 \equiv 0$ in the paraelectric phase under the absence of external field. So, the transition temperature from the paraelectric into the incommensurate ferroelectric phase is $T_{IC}(h)=T_C - \frac{2\alpha^S g_3}{\alpha_T h(\alpha^S\sqrt{g_3\varepsilon_0\varepsilon_{33}}+g_3)} + \frac{g_1^2}{4w_1\alpha_T}$. At fixed temperature T the transition thickness into the incommensurate phase is $h_{IC}(T) = \frac{-2\alpha^S g_3}{(\alpha_T(T-T_C)-g_1^2/4w_1)(\alpha^S\sqrt{g_3\varepsilon_0\varepsilon_{33}}+g_3)}$. These expressions are almost exact, since linear harmonic approximation is valid in the paraelectric phase ($T > T_{IC}$) as well as in the immediate vicinity of T_{IC}, where ferroelectric nonlinearity can be neglected.

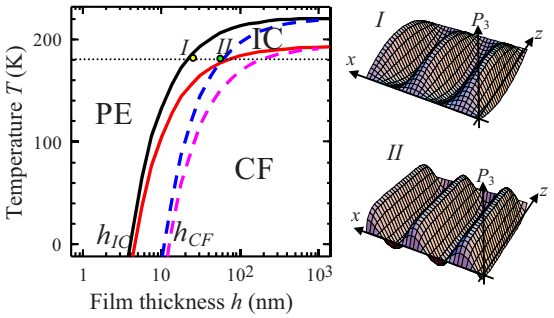

FIG. 2. (Color online). Phase diagram in the coordinates temperature-thickness of the film deposed on the matched substrate ($u_m^* \approx 0.003$) and placed between perfect conducting electrodes. PE is a paraelectric phase, IC is an incommensurate phase and CF is a commensurate ferroelectric phase. Solid and dashed curves correspond to the surface energy coefficient $\alpha^S=1$ and 10 m^2/F, respectively. Insets schematically show the polarization $\{x,z\}$ profiles in the points I and II of the phase diagram. Material parameters of $S_2P_2Se_6$: $\alpha_T=1.6\cdot10^6$ J·m/(C^2·K), $T_C=193$ K, $\beta=-4.8\cdot10^8$ J·m^5/C^4, $\gamma=8.5\cdot10^{10}$ J·m^9/C^6, $g_1=-5.7\cdot10^{-10}$ J·m^3/C^2, $w_1=1.8\cdot10^{-27}$ J·m^5/C^2, $v_1=1.2\cdot10^{-8}$ J·m^7/C^4, $g_3=5\cdot10^{-10}$ J·m^3/C^2, and positive $g_2 \sim g_3$ were taken from Refs. 61 and 62, $\varepsilon_{11}=\varepsilon_{33}=10$ (reference medium is isotropic dielectric).

The transition temperature into commensurate ferroelectric phase is $T_{CF}(h)=T_C - \frac{2\alpha^S g_3}{\alpha_T h(\alpha^S\sqrt{g_3\varepsilon_0\varepsilon_{33}}+g_3)}$. Note that $T_{IC}(h) = T_{CF}(h) + \frac{g_1^2}{4w_1\alpha_T}$ as anticipated.

At fixed temperature T the transition thickness into the commensurate phase is $h_{CF}(T) = \frac{-2\alpha^S g_3}{\alpha_T(T-T_C)(\alpha^S\sqrt{g_3\varepsilon_0\varepsilon_{33}}+g_3)}$. To our surprise numerical simulations showed that these expressions also appeared almost exact, most probably due to the same reasons as in commensurate ferroelectrics (see also Ref. 53 and next section).

Note, that the size-dependent term in $T_{CF}(h)$ and $T_{IC}(h)$, namely, $\frac{2\alpha^S g_3}{\alpha_T h(\alpha^S\sqrt{g_3\varepsilon_0\varepsilon_{33}}+g_3)}$, originates from the influence of depolarization field given by Eq. (1) and the finite surface energy ($\alpha^S \neq 0$). It is absent only for the unrealistic case without surface energy, when $\alpha^S=0$. Naturally, the depolarization field influence and finite surface energy determine the value of the transition thicknesses $h_{CF}(T)$ and $h_{IC}(T)$. The depolarization effect vanishes with the film thickness increase, i.e., at $h \gg h_{CF}(T)$.

As anticipated, Eq. (10) reduces to the well-known bulk solution $k_B^2(T) = -\frac{g_1}{2w_1} \pm \sqrt{\frac{g_1^2}{4w_1^2} - \frac{\alpha_T(T-T_C)}{w_1}}$ with the film thickness h increase. So, for the bulk sample the incommensurate modulation exists in the temperature range $T_C < T < T_{IC}$, where $T_{IC}=T_C + \frac{g_1^2}{4w_1\alpha_T}$ and $k_B^2(T_{IC}) = -g_1/2w_1$. Thus obtained analytical solution differs from the bulk solution in renormalization of α by depolarization field and surface effects, both contribute into finite-size effects.

Phase diagram in coordinates temperature—film thickness with paraelectric (PE), incommensurate (IC), and commensurate (CF) ferroelectric phases, and corresponding domain structure profiles are shown in Fig. 2.

It is seen from Fig. 2 that the transition temperatures into incommensurate and commensurate phases strongly depend

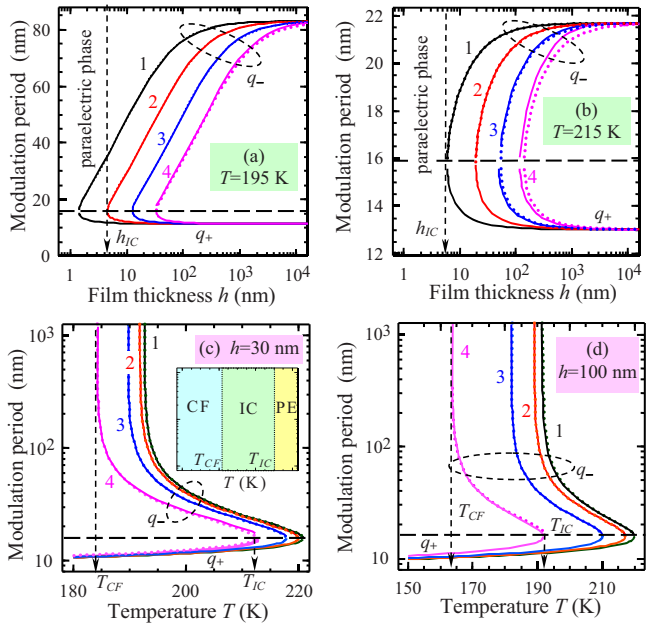

FIG. 3. (Color online). Thickness dependences of modulation periods $q_-=2\pi k_-^{-1}$ (top curves above the dashed horizontal line) and $q_+=2\pi k_+^{-1}$ (bottom curves below the dashed horizontal line) for different values of temperature (a) $T=195$ K and(b) 215 K. Temperature dependences of $q_-=2\pi k_-^{-1}$ (top curves) and $q_+=2\pi k_+^{-1}$ (bottom curves) for different values of the film thickness (c) $h=30$ nm and (d) 100 nm. Curves 1, 2, 3, and 4 correspond to the surface energy coefficient $\alpha^S=0.03$, 0.1, 0.3, and 1 m^2/F, respectively. Solid and dotted curves represent exact numerical calculations from Eqs. (7)–(9) and approximate analytical dependences (10), respectively. Material parameters are the same as in Fig. 2 and $R_d \sim 500$ nm.

on the film thickness due to the surface energy, depolarization field and polarization gradient, which contributions increases with the film thickness decrease. Thus "soft" incommensurate modulation appears at thickness $h_{IC}(T)$ and becomes "harder" with the thickness increase in CF phase (compare insets I and II plotted for thicknesses $h_I < h_{II}$).

Calculated modulation period $q_\pm(h,T)=2\pi k_\pm^{-1}(h,T)$ is presented in Fig. 3 for different values of the surface energy coefficient α^S (compare curves 1–4). It is seen that in the most cases approximate Eq. (10) (dotted curves) and numerical calculations from Eqs. (7)–(9) (solid curves) give almost the same results.

Summarizing results obtained in this section, we would like to underline that transition temperatures T_{CF}, T_{IC} and the maximal period $q_-=2\pi k_-^{-1}$ of the incommensurate domain structure strongly depend on the film thickness, depolarization field and surface energy contributions, while the minimal period $q_+=2\pi k_+^{-1}$ weakly depends on the film thickness. The correlation effects, which strength is in turn determined from the value of gradient coefficient g_1^*, determine the scale of both periods. The dependence of all polar properties on the Debye screening radius R_d is rather weak under the typical conditions $R_d \gg 50$ nm.

B. Phase-field modeling

In order to check the validity of the analytical calculations performed in harmonic approximation, we study the problem by the phase-field modeling.[63–65] Phase-field method allows rigorous numerical calculations of the spontaneous polarization spatial distribution and temporal evolution. The distribution of electric field is obtained by solving the electrostatic equations supplemented by the boundary conditions at the top and bottom electrodes. All-important energetic contributions (including depolarization field energy, electrostriction contribution, elastic energy, and surface energy) are incorporated into the total LGD free-energy functional $F(P_1,P_2,P_3,u_{ij})$. The temporal evolution of the polarization vector field, and thus the domain structure, is then described by the time-dependent LGD equations $\frac{\partial P_i}{\partial t}=-\Gamma\frac{\delta F}{\delta P_i}$, where Γ is the kinetic coefficient related to the domain-wall mobility. For a given initial distributions, numerical solution of the time-dependent LGD equations yields the temporal and spatial evolution of the polarization. We use periodic boundary conditions along both the x and y directions.

Approximate analytical results are compared with numerical phase-field calculations of 2D $\{x,y\}$-modulated domain structures in Figs. 4 for a thin film with dimensions $100\times100\times40$ nm at different temperatures. A positive surface energy coefficient α^S was employed. It is seen from the plots (b)–(e) that domain structure originated at low temperatures. So, the single domain state appeared unstable starting from much lower temperatures than T_{CF}. This supports the assumption made in Secs. V and I that domain stripes in ferroelectric phase possibly originate from finite surface energy value determined by nonzero α^S. It should be emphasized that periodic boundary conditions along both the x and y directions should affect the periodicity of the incommensurate structures.

Let us underline that phase field modeling results mimics labyrinth domain structures [see especially Figs. 4(b)–4(g)]. Possible qualitative explanation of the striking fact can be found in the Bjelis *et al.* papers,[66,67] where it was shown that the nonlinear Euler-Lagrange problem (3) without depolarization field and surface energy contribution represents an example of nonintegrable problem with chaotic phase portrait. Dananic *et al.* revealed that periodic solutions are isolated trajectories at the phase portrait in the uniaxial case and are physically trains of commensurate and incommensurate domains of various periods. Unfortunately the general results of Dananic and Bjelis cannot be applied quantitatively to the ferroelectric films on substrate considered in our paper, since they did not consider neither surface energy contribution nor depolarization field and strain effects (compare Eq. (2.2) in Ref. 66 with considered free energy (2)]. However it is well known that exactly depolarization field and surface energy contribution rule finite-size effects and size-induced phase transitions in spatially confined ferroelectrics.[2,5,6,8,15,20,25,30,45,53,54,59]

Additional numerical simulations proved that depolarization field decrease [reached by artificial increase of ε_{33} in Eq. (1) up to 10^2 and higher] and the second kind boundary conditions $\frac{\partial P_3}{\partial x_3}|_{x_3=0,h}=0$ (that exactly corresponds to the absence of surface energy, $\alpha^S=0$) strongly facilitate the spontaneous splitting on random domains in the considered system, while the depolarization field increase makes polarization distribution more ordered and eventually laby-

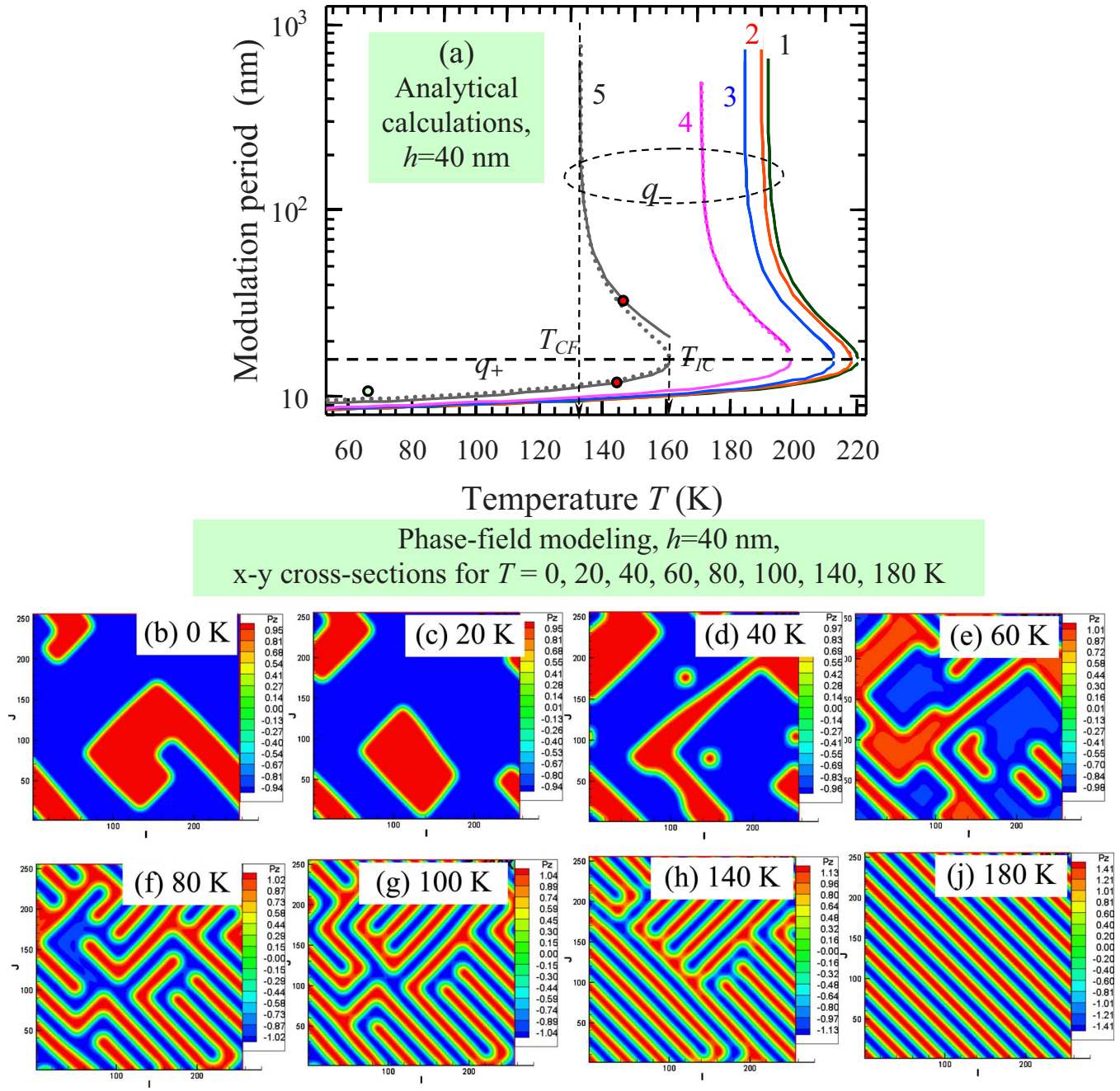

FIG. 4. (Color online). (a) Temperature dependence of the modulation period q_- (top curves above the dashed horizontal line) and q_+ (bottom curves below the dashed horizontal line) calculated analytically for the film thickness $h=40$ nm. Curves 1, 2, 3, 4, and 5 correspond to the surface energy coefficient $\alpha^S=0.03$, 0.1, 0.3, 1, and 10 m^2/F respectively. Solid and dotted curves represent numerical calculations from Eqs. (7)–(9) and approximate analytical dependences (10), respectively. (b)–(j) Temperature evolution of the $\{x,y\}$ modulated domain structure calculated by the phase-field modeling for the film with sizes $100\times100\times40$ nm, $\alpha^S=10$ m^2/F, and temperatures $T=0$, 20, 40, 60, 80, 100, 140, and 180 K. Other parameters are the same as in Fig. 2, but $g_2=g_1=-5.7\cdot10^{-10}$ $J\cdot m^3/C^2$ and $R_d\sim500$ nm.

rinthlike domains disappear. We also lead to the conclusion that the structures with mainly rectangular corners [shown in Figs. 4(b)–4(g)] possibly originate from the spatial confinement of the simulation volume in $\{x,y\}$-directions. However the structures only mimic true chaotic labyrinths with smooth random shapes. True labyrinthic domain structures appear near the surfaces of relaxor ferroelectrics [compare Fig. 1 from Ref. 68 and Fig. 2 from Ref. 69 with Figs. 4(b)–4(g)]. Relaxor ferroelectrics have anomalously high ε_{33} and accordingly very small depolarization fields are expected, therefore Dananic and Bjelis formalism may quantitatively describe their chaotic incommensurate domain structure.

We also performed 1D-phase field simulations to calculate the incommensurate x-modulated structures in thin plates with sizes $h_x=250$ nm, $h_y=2$ nm, $h_z=40$ nm. We calculated the polarization distribution at different temperatures [Fig. 5]. From Fig. 5 it can be seen that the P_3 distribution across

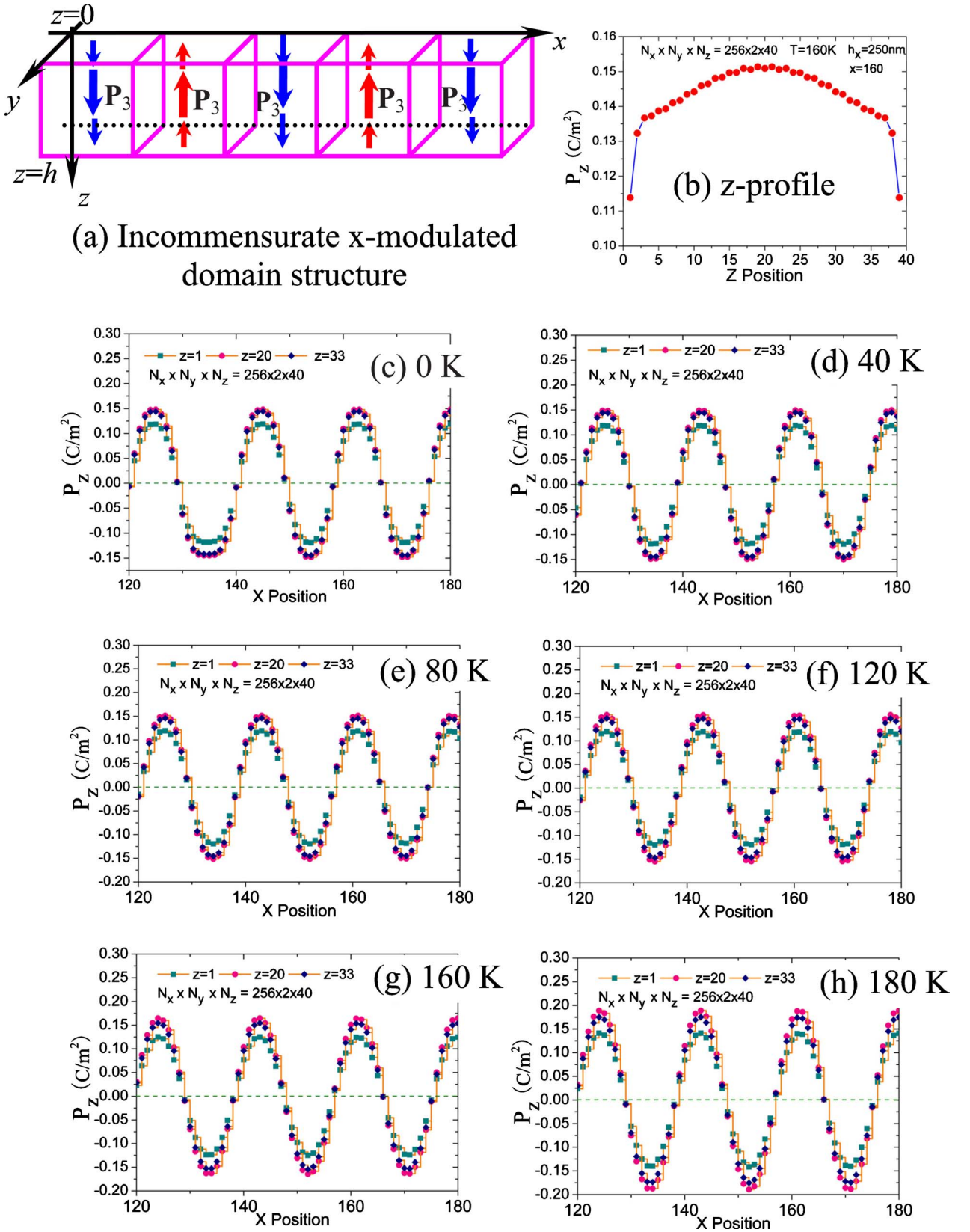

FIG. 5. (Color online). (a) Sketch of the 1D x-modulated domain structure. (b) Phase field 1D simulation of the polarization component P_3 variation for different z positions at $T=160$ K and $x=160$. (c)–(h) Polarization component P_3 morphologies in thin plates with sizes $h_x=250$ nm, $h_y=2$ nm, and $h_z=40$ nm at temperatures $T=0$, 40, 80, 120, 160, and 180 K. The pink solid circles, navy rhombus and dark cyan squares represent P_3 at $z=20$, 33, and 1, respectively. Other parameters are the same as in Fig. 4, but $g_1=-5.7\cdot10^{-10}$ J·m^3/C^2 and $g_2>0$.

the film depth z looks like a dome at fixed x position. P_3 is maximal in the middle of the film, and its module decreases from the middle to edges. Transversal x distribution of P_3 is periodic and it looks like sine wave with a period about 17.6 nm (18 grids) [Figs. 5(c)–5(h)]. This result provides necessary background for harmonic approximation used in Secs. IV and I in the deep enough incommensurate phase, i.e., at temperatures essentially lower than T_{IC}.

V. SUMMARY

We proposed the theoretical description of finite size, depolarization field effect, surface, and correlation energy influence on the phase diagram of thin ferroelectric films with II-type incommensurate phases and semiconductor properties.

Within the framework of Landau-Ginzburg-Devonshire theory we performed analytical calculations and phase-field modeling of the temperature evolution and thickness dependence of the period of incommensurate 180° domains appeared in thin films covered with perfect electrodes. Despite numerous efforts, the problem has not been solved previously.

It was shown analytically that the transition temperature between paraelectric, incommensurate, and commensurate ferroelectric phases (as well as the period of incommensurate domain structures) strongly depend on the film thickness, depolarization field contribution, surface energy and gradient coefficients. At the same time their dependences on Debye screening radius R_d are rather weak for the typical values $R_d \gg 50$ nm.

Unexpectedly, both the analytical theory and phase-field modeling results demonstrate that the incommensurate modulation can be stable in thin films in the wide temperature range starting from the low temperatures (much smaller than the bulk Curie temperature) up to the temperature of paraelectric phase transition. Phase field modeling results mimics labyrinth domain structures.

These domain stripes possibly originate even at low temperatures from the spatial confinement and finite surface energy contribution. Nonzero values of the surface energy lead to appearance of polarization inhomogeneity along the polar axis and depolarization field, localized near the surfaces. Similar effects could be the common feature of various confined ferroelectrics and ferromagnetics. Thus, we expect that the long-range order parameter (e.g., spontaneous polarization or magnetization) subjected to either spatial confinement or imperfect screening could reveal incommensurate modulation in nanosized ferroics. The result can be important for applications of the nanosized materials in nanoelectronics and memory devices.

We hope that our results would stimulate the experimental study of the size-induced phase transitions in thin ferroelectric films with incommensurate phase.

ACKNOWLEDGMENTS

Research sponsored by Ministry of Science and Education of Ukraine and National Science Foundation (Materials World Network, Grants No. DMR-0820404 and No. DMR-0908718).

*Corresponding author.
†morozo@i.com.ua
‡lqc3@psu.edu

[1] P. Bak, Rep. Prog. Phys. **45**, 587 (1982).
[2] R. Kretschmer and K. Binder, Phys. Rev. B **20**, 1065 (1979).
[3] E. V. Chensky and V. V. Tarasenko, Sov. Phys. JETP **56**, 618 (1982) [Zh. Eksp. Teor. Fiz. **83**, 1089 (1982)].
[4] J. Junquera and Ph. Ghosez, Nature (London) **422**, 506 (2003).
[5] A. N. Morozovska, M. D. Glinchuk, and E. A. Eliseev, Phys. Rev. B **76**, 014102 (2007).
[6] Q. Y. Qiu, V. Nagarajan, and S. P. Alpay, Phys. Rev. B **78**, 064117 (2008).
[7] C. W. Huang, Lang Chen, J. Wang, Q. He, S. Y. Yang, Y. H. Chu, and R. Ramesh, Phys. Rev. B **80**, 140101(R) (2009).
[8] Yue Zheng, C. H. Woo, and Biao Wang, J. Phys.: Condens. Matter **20**, 135216 (2008).
[9] C. Kittel, Phys. Rev. **70**, 965 (1946).
[10] T. Mitsui and J. Furuichi, Phys. Rev. **90**, 193 (1953).
[11] V. A. Zhirnov, Zh. Eksp. Teor. Fiz. **35**, 1175 (1959) [Sov. Phys. JETP **8**, 822 (1959)].
[12] W. Cao and L. E. Cross, Phys. Rev. B **44**, 5 (1991).
[13] A. M. Bratkovsky and A. P. Levanyuk, Phys. Rev. Lett. **86**, 3642 (2001).
[14] W. T. Lee, E. K. H. Salje, and U. Bismayer, Phys. Rev. B **72**, 104116 (2005).
[15] I. A. Luk'yanchuk, A. Schilling, J. M. Gregg, G. Catalan, and J. F. Scott, Phys. Rev. B **79**, 144111 (2009).
[16] D. D. Fong, G. B. Stephenson, S. K. Streiffer, J. A. Eastman, O. Auciello, P. H. Fuoss, and C. Thompson, Science **304**, 1650 (2004).
[17] C. Lichtensteiger, J.-M. Triscone, J. Junquera, and P. Ghosez, Phys. Rev. Lett. **94**, 047603 (2005).
[18] G. B. Stephenson and K. R. Elder, J. Appl. Phys. **100**, 051601 (2006).
[19] V. Nagarajan, J. Junquera, J. Q. He, C. L. Jia, R. Waser, K. Lee, Y. K. Kim, S. Baik, T. Zhao, R. Ramesh, Ph. Ghosez, and K. M. Rabe, J. Appl. Phys. **100**, 051609 (2006).
[20] E. A. Eliseev, A. N. Morozovska, C V. Kalinin, Y. L. Li, Jie Shen, M. D. Glinchuk, L. Q. Chen, and V. Gopalan, J. Appl. Phys. **106**, 084102 (2009).
[21] S. Prosandeev, I. Ponomareva, I. Kornev, I. Naumov, and L. Bellaiche, Phys. Rev. Lett. **96**, 237601 (2006).
[22] P. Aguado-Puente and J. Junquera, Phys. Rev. Lett. **100**, 177601 (2008).
[23] G. Catalan, A. Schilling, J. F. Scott, and J. M. Gregg, J. Phys.: Condens. Matter **19**, 132201 (2007).
[24] A. Gruverman, D. Wu, H.-J. Fan, I. Vrejoiu, M. Alexe, R. J. Harrison, and J. F. Scott, J. Phys.: Condens. Matter **20**, 342201 (2008).
[25] I. A. Luk'yanchuk, L. Lahoche, and A. Sené, Phys. Rev. Lett.

102, 147601 (2009).
[26] D. A. Scrymgeour, V. Gopalan, A. Itagi, A. Saxena, and P. J. Swart, Phys. Rev. B **71**, 184110 (2005).
[27] D. Lee, R. K. Behera, P. Wu, H. Xu, S. B. Sinnott, S. R. Phillpot, L. Q. Chen, and V. Gopalan. Phys. Rev. B **80**, 060102(R) (2009).
[28] W. Selke, D. Catrein, and M. Pleimling, J. Phys. A **33**, L459 (2000).
[29] W. Selke, M. Pleimling, and D. Catrein, Eur. Phys. J. B **27**, 321 (2002).
[30] D. R. Tilley, *Finite-size Effects on Phase Transitions in Ferroelectrics in Ferroelectic Thin Films*, edited by C. Paz de Araujo, J. F. Scott, and G. W. Teylor (Gordon and Breach, New York, 1996).
[31] J. d'Albuquerque e Castro, D. Altbir, J. C. Retamal, and P. Vargas, Phys. Rev. Lett. **88**, 237202 (2002).
[32] W. Zhang and S. Haas, J. Magn. Magn. Mater. **321**, 3687 (2009).
[33] Yu. V. Sereda, Phys. Rev. B **66**, 054109 (2002).
[34] A. V. Babich, S. V. Berezovsky, V. F. Klepikov, and Yu. V. Sereda, Condens. Matter Phys. **9**, 121 (2006).
[35] S. V. Berezovsky, V. Yu. Korda, and V. F. Klepikov, Phys. Rev. B **64**, 064103 (2001).
[36] E. V. Charnaya, S. A. Ktitorov, and O. S. Pogorelova, Ferroelectrics **297**, 29 (2003).
[37] A. P. Levanyuk, S. A. Minyukov, and A. Cano, Phys. Rev. B **66**, 014111 (2002).
[38] G. H. F. van Raaij, K. J. H. van Bemmel, and T. Janssen, Phys. Rev. B **62**, 3751 (2000).
[39] K. Z. Rushchanskii, Y. M. Vysochanskii, and D. Strauch, Phys. Rev. Lett. **99**, 207601 (2007).
[40] C.-G. Duan, S. S. Jaswal, and E. Y. Tsymbal, Phys. Rev. Lett. **97**, 047201 (2006).
[41] G. Geneste, E. Bousquest, J. Junquera, and P. Ghosez, Appl. Phys. Lett. **88**, 112906 (2006).
[42] M. Q. Cai, Y. Zheng, B. Wang, and G. W. Yang, Appl. Phys. Lett. **95**, 232901 (2009).
[43] J. W. Hong, G. Catalan, D. N. Fang, Emilio Artacho, and J. F. Scott, arXiv:0908.3617 (unpublished).
[44] C. L. Wang and S. R. P. Smith, J. Phys.: Condens. Matter **7**, 7163 (1995).
[45] A. N. Morozovska, E. A. Eliseev, and M. D. Glinchuk, Phys. Rev. B **73**, 214106 (2006).
[46] A. Sundaresan, R. Bhargavi, N. Rangarajan, U. Siddesh, and C. N. R. Rao, Phys. Rev. B **74**, 161306(R) (2006).
[47] D. Yadlovker and Sh. Berger, Phys. Rev. B **71**, 184112 (2005).
[48] D. Yadlovker and Sh. Berger, Appl. Phys. Lett. **91**, 173104 (2007).
[49] D. Yadlovker and Sh. Berger, J. Appl. Phys. **101**, 034304 (2007).
[50] E. Erdem, H.-Ch. Semmelhack, R. Bottcher, H. Rumpf, J. Banys, A. Matthes, H.-J. Glasel, D. Hirsch, and E. Hartmann, J. Phys.: Condens. Matter **18**, 3861 (2006).
[51] The dependence of ε_{11} on E_3 is absent for uniaxial ferroelectrics. It may be essential for perovskites with high coupling constant.
[52] A. N. Morozovska, E. A. Eliseev, JianJun Wang, G. S. Svechnikov, Yu. M. Vysochanskii, Venkatraman Gopalan, and Long-Qing Chen, arXiv:0912.4423 (unpublished).
[53] M. D. Glinchuk, E. A. Eliseev, V. A. Stephanovich, and R. Farhi, J. Appl. Phys. **93**, 1150 (2003).
[54] M. D. Glinchuk, A. N. Morozovska, and E. A. Eliseev, J. Appl. Phys. **99**, 114102 (2006).
[55] N. A. Pertsev, A. G. Zembilgotov, and A. K. Tagantsev, Phys. Rev. Lett. **80**, 1988 (1998).
[56] Note that the renormalization does not contribute into the equations of state in a single-domain sample with constant polarization $P_0(x,y,z)=\bar{P}_0$, since $\alpha'\bar{P}_0+\beta'\bar{P}_0^3 \equiv \alpha\bar{P}_0+\beta\bar{P}_0^3$.
[57] J. S. Speck and W. Pompe, J. Appl. Phys. **76**, 466 (1994).
[58] C.-L. Jia and Valanoor Nagarajan, J.-Q. He, L. Houben, T. Zhao, R. Ramesh, K. Urban, and R. Waser, Nat. Mater. **6**, 64 (2007).
[59] M. D. Glinchuk, E. A. Eliseev, A. Deineka, L. Jastrabik, G. Suchaneck, T. Sandner, G. Gerlach, and M. Hrabovsky, Integr. Ferroelectr. **38**, 101 (2001).
[60] M. I. Kaganov and A. N. Omelyanchouk, Zh. Eksp. Teor. Fiz. **61**, 1679 (1971) [Sov. Phys. JETP **34**, 895 (1972)].
[61] Yu. M. Vysochanskii, M. M. Mayor, V. M. Rizak, V. Yu. Slivka, and M. M. Khoma, Zh. Eksp. Teor. Fiz. **95**, 1355 (1989) [Sov. Phys. JETP **68**, 782 (1989)].
[62] M. M. Khoma, A. A. Molnar, and Yu. M. Vysochanskii, J. Phys. Stud. **2**, 524 (1998).
[63] Y. L. Li, S. Y. Hu, Z. K. Liu, and L. Q. Chen, Appl. Phys. Lett. **78**, 3878 (2001).
[64] Y. L. Li, S. Y. Hu, Z. K. Liu, and L. Q. Chen, Acta Mater. **50**, 395 (2002).
[65] S. V. Kalinin, A. N. Morozovska, L. Q. Chen, and B. J. Rodriguez, Rep. Prog. Phys. **73**, 056502 (2010).
[66] V. Dananic and A. Bjelis, Phys. Rev. E **50**, 3900 (1994).
[67] V. Dananic, A. Bjelis, M. Rogina, and E. Coffou, Phys. Rev. A **46**, 3551 (1992).
[68] S. V. Kalinin, B. J. Rodriguez, S. Jesse, A. N. Morozovska, A. A. Bokov, and Z.-G. Ye, Appl. Phys. Lett. **95**, 142902 (2009).
[69] S. V. Kalinin, B. J. Rodriguez, J. D. Budai, S. Jesse, A. N. Morozovska, A. A. Bokov, and Z.-G. Ye, Phys. Rev. B **81**, 064107 (2010).